Oxidation and aging in U and Pu probed by spin-orbit sum rule analysis: Indications for covalent metal-oxide bonds

K. T. Moore,[1,*] G. van der Laan,[2] R. G. Haire,[3] M. A. Wall,[1] and A. J. Schwartz[1]

[1]*Lawrence Livermore National Laboratory, Livermore, California 94550, USA*
[2]*Magnetic Spectroscopy Group, Daresbury Laboratory, Warrington WA4 4AD, United Kingdom*
[3]*Oak Ridge National Laboratory, MS-6375, Oak Ridge, Tennessee 37831, USA*

Transmission electron microscopy is used to acquire electron energy-loss spectra from phase-specific regions of Pu and U metal, PuO_2 and UO_2, and aged, self-irradiated Pu metal. The $N_{4,5}$ ($4d \rightarrow 5f$) spectra are analyzed using the spin-orbit sum rule. Our results show that the technique is sensitive enough to detect changes in the branching ratio of the white-line peaks between the metal and dioxide of both U and Pu. There is a small change in the branching ratio between different Pu metals, and the data trends as would be expected for varying f electron localization, i.e., α-Pu, δ-Pu, and aged δ-Pu. Moreover, our results suggest that the metal-oxide bonds in UO_2 and PuO_2 are strongly covalent in nature and do not exhibit an integer valence change as would be expected from purely ionic bonding.

PACS number(s): 71.27.+a, 71.70.−d, 71.10.−w, 78.70.Dm

Actinide physics and chemistry are of great interest due to the unique behavior of the $5f$ states that dominate the electronic structure.[1–6] How these states evolve with changes in crystal structure,[7,8] alloying,[9,10] and oxidation state[11,12] is of considerable importance to better understand these materials. In particular, oxidation states have been an intriguing and often hotly debated topic for the actinides. Recent results in actinide chemistry have shown that the behavior of solid-state actinide oxides has considerable similarities to molecular systems.[13,14] These studies suggest that the metal-oxide bonds are appreciably covalent in nature. If correct, the metal-oxide bonds would not represent an integer change in valence.

Another important question for actinides is how the electronic structure changes due to the accumulation of damage via self-irradiation. It is known that He atoms, vacancies, and interstitials are introduced into the lattice due to the α decay of Pu, and that He bubbles form and grow with time.[15] When these defects are introduced, the lattice expands, and this should produce an increased localization of the f states in comparison to newly produced Pu with few defects. Being able to measure any changes in the electronic structure as a function of age would be tantamount for understanding the behavior of the material with time.

A powerful tool for interrogating the $5f$ states is the spin-orbit sum rule,[16,17] which works particularly well for the actinides as an unambiguous probe for the $5f$ spin-orbit interaction per hole.[18,19] In order to use the spin-orbit sum rule, the branching ratio must first be extracted from the spin-orbit split white-lines of spectra; in our case recorded by electron energy-loss spectroscopy (EELS) in a transmission electron microscope (TEM). This technique permits the use of a nanometer-sized probe to collect spectra and diffraction patterns from phase-specific regions of samples. It has been shown repeatedly that EELS acquired at high accelerating voltages, such as used here, are equivalent to x-ray absorption spectroscopy measurements,[7,20,21] i.e., the spectra can be analyzed in exactly the same manner.

Buck and Fortner *et al.*[11,22,23] have produced a considerable amount of data for Th, U, and Pu materials using the branching ratio of the $M_{4,5}$ edge. They too employed EELS in a TEM, which is no easy task given the small amount of intensity yielded by this technique at ~3.5 keV where the $M_{4,5}$ ionization edges for the actinides are found. Their data showed that the $M_{4,5}$ edge is quite sensitive to changes in the environment of the actinide element, producing changes in the branching ratio for various f-electron materials.

Using the $N_{4,5}$ edge for Th, U, and Pu metals it has been shown that there is a connection between the expectation value of the angular part of the spin-orbit parameter and the degree of $5f$ localization.[4,18] In the case of U, which has delocalized $5f$ states, the spin-orbit sum rule indicates an LS coupling mechanism. However, in the case of Pu, which has more localized $5f$ states, the spin-orbit sum rule indicates an intermediate coupling scheme. The previous research[18] was focused on the applicability of the spin-orbit sum rule to the ground-state phases of each metal. This technique has yet to be extended to the oxidation and aging of actinide metals or to the numerous allotropic phases that occur in each metal.

In this Brief Report we employ the spin-orbit sum rule to examine the actinide elements U and Pu in the metallic and dioxide form, and aged δ-Pu with considerable damage due to self-irradiation. Our data show that the branching ratio of the $N_{4,5}$ ($4d \rightarrow 5f$) EELS spectra, and in turn the spin-orbit sum rule, is sensitive enough to detect differences between the dioxide and metal forms of both U and Pu. There is a minor difference between plutonium metals, and the data trends in the correct manner based on f-electron localization; α-Pu, δ-Pu, aged δ-Pu. Finally, our results suggest that the bonding in UO_2 and PuO_2 is strongly covalent in nature and does not exhibit an integer valence change as would be expected from ionic bonding.

The samples used in these experiments were single crystal UO_2, α-U, PuO_2, α-Pu, α'-Pu (where the prime denotes Ga in the lattice), Ga-stabilized δ-Pu, aged Ga-stabilized δ-Pu, and AmH_2. All Pu samples were less than three years old except for the aged Ga-stabilized δ-Pu alloy, which was 44 years old at the time of analysis. The Ga content for all

TABLE I. The Ga content in wt. % for samples containing gallium, the perceived f-electron count, the branching ratio B of the $N_{4,5}$ EELS spectra, and the expectation value of the $5f$ spin-orbit interaction per hole $\langle w^{110}\rangle/n_h$ for each material examined. The sum rule requires a small correction factor, which is $\Delta=-0.010$, 0, and 0.005 for $n=3$, 5.4, and 6, respectively (Ref. 18).

	Ga content wt. %	f count	Branching ratio (B)	$\dfrac{\langle w^{110}\rangle}{n_h}-\Delta$
α-U		3 (Refs. 11,16)	0.686 (002)	−0.215 (005)
UO$_2$		3	0.729 (001)	−0.3225 (0005)
α-Pu new		5.4 (Ref. 6)	0.843 (010)	−0.6075 (0250)
α'-Pu new	0.6	5.4 (Ref. 6)	0.842 (006)	−0.605 (015)
δ-Pu new	0.6	5.4 (Ref. 6)	0.847 (005)	−0.6174 (0126)
δ-Pu aged	1.0	5.4 (Ref. 6)	0.856 (NA)	−0.64
PuO$_2$	0.6	5.4 (Ref. 6)	0.874 (014)	−0.685 (035)
AmH$_2$		6	0.928 (008)	−0.82 (020)

newer Pu alloys is 0.6 wt. %, while the aged alloy is 1.0 wt. % (see Table I). The UO$_2$ sample was a large single crystal with close to perfect stoichiometry. PuO$_2$ was grown in the TEM by allowing the sample to oxidize over several days. A TEM image of the oxidation front is shown in the inset of Fig. 1(b). The diffraction pattern in the upper-left of the inset shows that the oxide is polycrystalline with some texture, as evidenced by the bumpy intensity distribution in each diffraction ring. Measuring the rings yields a d-spacing that matches exactly with a face-centered cubic form of PuO$_2$ ($a=5.396$ Å). EELS spectra revealed a nitrogen edge, indicating that there was some substitution of nitrogen for oxygen in the PuO$_2$ lattice.

EELS experiments were performed using a Philips CM300 field-emission-gun TEM operating at 297 keV and a Gatan image filter. Spectra were collected using a sample thickness of ~0.5 inelastic mean free path (~40 nm), as calculated by the ratio of the zero-loss peak to the plasmon peak. Background removal was performed with an inverse power-law extrapolation, and these spectra were used for illustration purposes. For branching ratio analysis the second derivative of the *raw* spectra was calculated and the area beneath the N_5 ($4d_{5/2}$) and N_4 ($4d_{3/2}$) peaks was integrated above zero.[24] This technique is beneficial, since it reduces the signal-to-noise ratio in the spectrum and circumvents the need to remove the background intensity with an inverse power-law extrapolation as described above. An example of this is shown in the inset in Fig. 1(c), where the gray areas indicate the integrated regions used for branching ratio analysis. The branching ratio $B=I(N_5)/[I(N_5)+I(N_4)]$ was obtained as described in Ref. 18, where $I(N_5)$ and $I(N_4)$ are the integrated intensity of the N_5 and N_4 peaks, respectively.

The spectra for the U and Pu materials are shown in Figs. 1(a)–1(c). For both elements the dioxide has a smaller N_4 peak than the metal, i.e., the branching ratio is larger for the dioxide (see Table I). In addition, the dioxide peaks are narrower in relation to the metals. For UO$_2$ the N_5 and N_4 peaks are 5.2 eV wide at full-width half maximum, while the peaks are 5.8 eV for α-U. For PuO$_2$ the peaks are 6.0 eV wide, while they measure 7.0 eV for α'- and δ-Pu.

Both α'- and δ-Pu in Fig. 1(b) have similar spectra with only a small difference in the branching ratio (see Table I). Each of these metals are new with minor self-irradiation damage and have the same Ga content, since the α' phase was formed from δ via the isothermal martensitic transformation that occurs at ~−120 °C.[2] Although not shown, new, unalloyed α-Pu exhibits a similar spectra with almost the same branching ratio as α'-Pu (see Table I).

The aged δ-Pu sample, which had accumulated appreciable defects and He bubbles due to self-irradiation,[15] showed a more considerable increase in branching ratio compared to new α-, new α'-, and new δ-Pu. Examining Fig. 1(c), the N_4 peak for aged δ-Pu is slightly smaller than that of the new δ-Pu. There is a broad hump in the spectra between the N_5 and N_4 peaks that we do not presently understand. The possibility of Am in the aged sample was considered, but the Am N_5 peak is centered at ~830 eV rather than ~823 eV and there should not be enough Am in the sample to be detected via EELS.

We may now use the branching ratios from the spectra in Fig. 1, and listed in Table I, for sum-rule analysis, which yields the values of the spin-orbit interaction per hole. For the f shell, the expectation value of the angular part of the spin-orbit parameter is $\langle w^{110}\rangle=2/3 \ \langle l \cdot s\rangle=n_{7/2}-4/3 \ n_{5/2}$, where $n_{7/2}$ and $n_{5/2}$ are the electron occupation numbers for the angular-momentum levels $j=7/2$ and $5/2$.[18,19] Thus, $\langle w^{110}\rangle$ reveals the proper angular momentum coupling scheme for a given material. For the $d \rightarrow f$ transition, the sum rule gives the spin-orbit interaction per hole as

$$\frac{\langle w^{110}\rangle}{n_h}-\Delta=-\frac{5}{2}\left(B-\frac{3}{5}\right), \qquad (1)$$

where B is the branching ratio for the experimental spectra, n_h is the number of holes in the f shell, and Δ represents the small correction term for the sum rule as given in Table II of Ref. 18. This correction term has been calculated using Cowan's relativistic Hartree-Fock code[25] taking into account Coulomb, exchange, and spin-orbit interactions on equal footings.[19] Table I lists the spin-orbit interaction per number of holes minus the correction term, $w^{110}/n_h-\Delta$, for each material analyzed.

To better visualize the data, a plot of $w^{110}/n_h-\Delta$ as a function of the number of f electrons is shown in Fig. 2. Within this plot the three theoretical angular momentum coupling schemes are drawn: LS, jj, and intermediate. The number of f electrons in actinide metals and compounds has always been a difficult and intensely debated subject. The spin-orbit sum rule does not yield the f count, so we assign the $5f$-electron count via guidance by literature and by the fact that oxides, as localized systems, should be directly on the
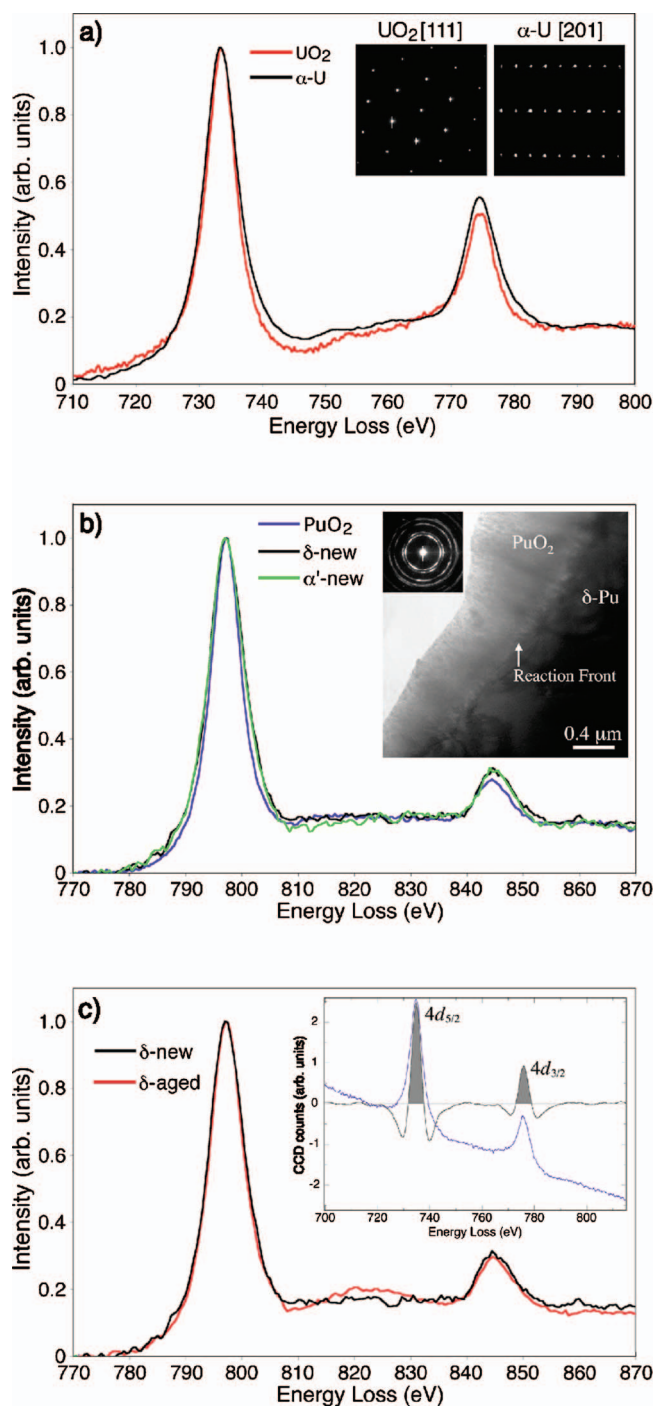
FIG. 1. (Color) EELS spectra for U (a) and Pu [(b) and (c)]. For U and UO$_2$ (a), there are two single-crystal diffraction patterns inset that verify the phase being examined by EELS. (b) The spectra for α'-Pu, δ-Pu, and PuO$_2$. A TEM image of the δ-Pu sample that oxidized in the TEM over several days to produce PuO$_2$ is shown in the inset of (b). (c) The EELS spectra for new and aged δ-Pu. A compound graph of a raw $N_{4,5}$ EELS spectrum and the second derivative of that spectrum is inset in (c), showing how the area beneath each peak was extracted and integrated.

intermediate coupling curve.[16] Thus, U is assumed as $f=3$ (Refs. 11 and 16) and Pu as $f=5.4$.[6] As previously observed,[18] α-U falls near the LS coupling curve while Pu
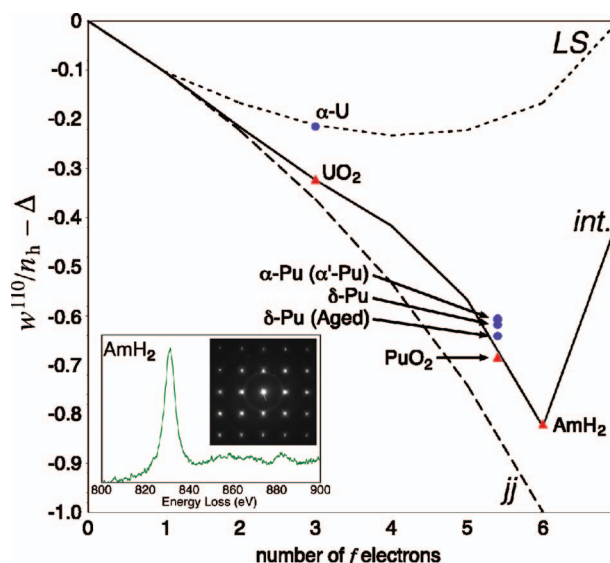

FIG. 2. (Color) A plot of w^{110}/n_h-Δ as a function of the number of f electrons. The three theoretical angular momentum coupling schemes are shown: LS, jj, and intermediate coupling. Metals and alloys are indicated by blue circles and dioxides and hydrides by red triangles. The AmH$_2$ $N_{4,5}$ EELS edge is shown in the lower-left inset, accompanied by a [100] diffraction pattern.

falls near the intermediate coupling curve, where the large change in electron coupling behavior is due to the delocalized nature of the 5f states in U compared to the localized nature of the 5f states in Pu. These results have been previously examined in detail in Ref. 18 and will not be discussed here. The new pieces of data are that both UO$_2$ and PuO$_2$ have a lower $w^{110}/n_h-\Delta$ value than their metal forms due to a increase in the branching ratio. The striking feature here is our choice of the number of f electrons for each dioxide material. If a purely ionic transfer of charge occurred, U should be f^2, having given up four electrons: the $(spd)^3$ and one f electron. Likewise, Pu should be f^4 having given up four electrons: $(spd)^{2.6}$ and $f^{1.4}$. However, if we plot the oxides with this number of f electrons, we find that they are outside the jj coupling limit. This is not physically possible, since jj coupling corresponds to the extreme case where all electrons go into the $j=5/2$ level, until this level is full. With this in mind, we propose the avant-garde idea that UO$_2$ and PuO$_2$ do not have an f^2 and f^4 configuration, respectively. Rather, each element retains a similar f-electron count in the dioxide as the metal due to covalent metal-oxide bonding. In reality, the f count certainly drops a fraction due to some degree of ionic character in the bonding. However, for clarity we plot the f-electron count for the oxides the same as the metal and do not try to guess the ionic-covalent fraction. In the end, the point is that the spin-orbit sum rule applied to the experimental branching ratios shows that an integer valence change is not physically reasonable.

Recent experiments in actinide chemistry suggest that the behavior of solid-state actinide oxides shows significant similarities to molecular systems,[13,14] meaning that the metal-oxide bonds are covalent in nature. If this is indeed the case, then the materials would not exhibit an integer transfer of ionic charge. Rather, the metal-oxide bonds would share

the electron charge. Judging by the branching ratio and subsequent spin-orbit analysis, our results support the actinide chemistry results that the bonding in UO_2 and PuO_2 has an appreciably covalent nature and that the f-electron count remains similar to that of the metal.

X-ray absorption experiments with full multiple-scattering (MS) simulations of the O K edge of UO_2 (Refs. 26 and 27) and photoemission spectroscopy[28] have both indicated covalent bonding between uranium and oxygen. In each case the O $2p$ band had appreciable $5f$ character, which is indicative of covalent bonding.

X-ray and ultraviolet photoelectron spectroscopy of Am thin films[29] also showed no difference between the AmN, AmSb, and Am_2O_3 spectra, each being consistent with a $5f^6$ ground-state configuration. Normally nitrides and antimonides are more covalent than oxides, but again we see that the oxide is exhibiting considerable covalent nature. As one further data set, we measured the branching ratio from EELS (see inset in Fig. 2) and calculated $w^{110}/n_h - \Delta$ for AmH_2 (fcc, $a = 5.348$ Å). If we accept any integer number less than $f = 6$, we find $w^{110}/n_h - \Delta$ would fall beyond the jj limit, which again is not physically possible. The lowest f count possible with the observed $w^{110}/n_h - \Delta$ value would be 5.4.

Another important piece of information yielded by Fig. 2 is that the trend of the $w^{110}/n_h - \Delta$ values for Pu metals and alloys is just as one would expect: α-Pu and α'-Pu have the highest value, Ga-stabilized δ-Pu is slightly lower, and finally, aged, Ga-stabilized δ-Pu has the lowest value. The α phase is much denser crystallographically and is broadly accepted to have the strongest f-electron hybridization. Thus, it should be the closest to the LS limit. δ-Pu, which has a considerably expanded lattice compared to α and correspondingly more localized f states, falls closer to the jj limit. Finally, aged, Ga-stabilized δ-Pu falls the closest to the jj limit of all the Pu metals. This is a physically acceptable result, since the aged lattice is expanded due to accumulated damage from self-irradiation, further localizing the f states. While the standard deviations just overlap numerically for the Pu results, the trend in data was reproducible over numerous areas of each sample, giving further confidence in the data. Thus, EELS in a TEM and the spin-orbit sum rule may represent an experimental technique sensitive enough to detect changes in the *bulk* electronic structure of actinide metals caused by self-irradiation damage.

The Ga content in the Pu sample must also be considered, since it affects the lattice. All Pu-Ga samples contain 0.6 wt. % Ga except the aged sample, which had 1.0 wt. % Ga. Since the aged sample shows the largest change in $w^{110}/n_h - \Delta$ value of the Pu metals and alloys, it exposes the need in future experiments to systematically examine the branching ratio and spin-orbit interaction of Pu as a function of Ga content. It is worthy of note, however, that both α-Pu with no Ga and α'-Pu with 0.6 wt. % Ga have an almost identical $w^{110}/n_h - \Delta$ value, suggesting no considerable dependence on Ga concentration.

In summary, we have used the branching ratio of the $N_{4,5}$ EELS edge and the spin-orbit sum rule for U and Pu metal, UO_2 and PuO_2, and aged, self-irradiated Pu metal. Our results show that the branching ratio, and in turn the spin-orbit sum rule, is sensitive enough to detect changes between the metal and dioxide forms of U and Pu. The branching ratio changes between each of the Pu metals, and the data trends in the correct fashion; α- and α'-Pu, δ-Pu, aged δ-Pu, where α-Pu is closest to the LS limit and aged δ-Pu is closest to the jj limit. Thus, EELS and the spin-orbit sum rule could be used a probe for tracking changes in the electronic structure due to self-irradiation damage with time. Finally, the spin-orbit analysis suggests that UO_2 and PuO_2 have a valence near that of the U and Pu metal, respectively, i.e., there is a considerable covalent nature in the metal-oxide bonds. This idea has recently come to the forefront of actinide chemistry, and our data supports the assertion.

---

*Contact author: Tel: 925-422-9741, Fax: 925-422-6892, Email: moore78@llnl.gov

[1] R. C. Albers, Nature (London) **410**, 759 (2001).
[2] S. S. Hecker, Metall. Mater. Trans. A **35**, 2207 (2004).
[3] H. L. Skrivers *et al.*, Phys. Rev. Lett. **41**, 42 (1978).
[4] J. G. Tobin *et al.*, Phys. Rev. B **72**, 085109 (2005).
[5] S. Y. Savrasov *et al.*, Nature (London) **410**, 793 (2001).
[6] L. Havela *et al.*, Phys. Rev. B **65**, 235118 (2002).
[7] K. T. Moore *et al.*, Phys. Rev. B **69**, 193104 (2004).
[8] K. T. Moore *et al.*, Philos. Mag. **84**, 1039 (2004).
[9] T. Gouder *et al.*, Phys. Rev. B **71**, 165101 (2005).
[10] P. G. Allen *et al.*, Phys. Rev. B **65**, 214107 (2002).
[11] M. Colella *et al.*, Phys. Chem. Miner. **32**, 52 (2005).
[12] P. G. Allen *et al.*, Inorg. Chem. **36**, 4676 (1997).
[13] C. J. Burns, Science **309**, 1823 (2005).
[14] S. D. Conradson *et al.*, J. Am. Chem. Soc. **126**, 13443 (2004).
[15] A. J. Schwartz *et al.*, Philos. Mag. **85**, 479 (2005).
[16] G. van der Laan and B. T. Thole, Phys. Rev. Lett. **60**, 1977 (1988).
[17] B. T. Thole and G. van der Laan, Phys. Rev. B **38**, 3158 (1988).
[18] G. van der Laan *et al.*, Phys. Rev. Lett. **93**, 097401 (2004).
[19] G. van der Laan and B. T. Thole, Phys. Rev. B **53**, 14 458 (1996).
[20] G. Blanche *et al.*, Ultramicroscopy **50**, 141 (1993).
[21] K. T. Moore *et al.*, Phys. Rev. Lett. **90**, 196404 (2003).
[22] E. C. Buck and J. A. Fortner, Ultramicroscopy **67**, 69 (1997).
[23] J. A. Fortner and E. C. Buck, Appl. Phys. Lett. **68**, 3817 (1996).
[24] D. B. Williams and C. B. Carter, *Transmission Electron Microscopy—A Textbook for Materials Science* (Plenum, New York, 1996).
[25] R. D. Cowan, *The Theory of Atomic Structure and Spectra* (University of California Press, Berkeley, 1981).
[26] F. Jollet *et al.*, J. Phys.: Condens. Matter **9**, 9393 (1997).
[27] Z. Y. Wu *et al.*, J. Phys.: Condens. Matter **11**, 7185 (1999).
[28] J. R. Naegele *et al.*, Struct. Bonding (Berlin) **59–60**, 197 (1985).
[29] T. Gouder *et al.*, Phys. Rev. B **72**, 115122 (2005).